MOLECULAR AND CELLULAR BIOLOGY, Aug. 1985, p. 1901–1909
0270-7306/85/081901-09$02.00/0

Vol. 5, No. 8

Suppressors of *Saccharomyces cerevisiae his3* Promoter Mutations Lacking the Upstream Element

MARJORIE A. OETTINGER AND KEVIN STRUHL*

Department of Biological Chemistry, Harvard Medical School, Boston, Massachusetts 02115

Received 15 February 1985/Accepted 7 May 1985

Transcription of the *Saccharomyces cerevisiae his3* gene requires an upstream promoter element and a TATA element. A strain containing *his3*-Δ13, an allele which deletes the upstream promoter element but contains the TATA box and intact structural gene, fails to express the gene and consequently is unable to grow in medium lacking histidine. In this paper we characterize His$^+$ revertants of *his3*-Δ13 which are due to unlinked suppressor mutations. Recessive suppressors in three different *ope* genes allow *his3*-Δ13 to be expressed at wild-type levels. In all cases, the suppression is due to increased *his3* transcription. However, unlike the wild-type *his3* gene, whose transcripts are initiated about equally from two different sites (+1 and +12), transcription due to the *ope* mutations is initiated only from the +12 site. *ope*-mediated transcription is regulated in a novel manner; it is observed in minimal medium, but not in rich broth. Although *ope* mutations restore wild-type levels of transcription, *his3* chromatin structure, as assayed by micrococcal nuclease sensitivity of the TATA box, resembles that found in the *his3*-Δ13 parent rather than in the wild-type strain. This provides further evidence that TATA box sensitivity is not correlated with transcriptional activation. *ope* mutations are pleiotropic in that cells have a crunchy colony morphology and lyse at 37°C in conditions of normal osmolarity. *ope* mutations are allele specific because they fail to suppress five other *his3* promoter mutations. We discuss implications concerning upstream promoter elements and propose some models for *ope* suppression.

Transcription of eucaryotic genes by RNA polymerase II requires at least two distinct promoter elements (1, 4–6, 8, 11, 12, 20). One element, the TATA box, is a highly conserved sequence found before essentially all eucaryotic structural genes (reviewed in reference 3). It is also similar in sequence to the Pribnow box, a binding site for *Escherichia coli* RNA polymerase (reviewed in reference 9). The TATA element is usually located a fixed distance from the transcriptional start site and is sufficient to direct accurate transcriptional initiation in vitro (7, 10). These observations have led to the general view that RNA polymerase or an associated factor binds to the TATA sequence and directly results in the initiation of RNA synthesis.

Sequences more than 100 base pairs upstream of the initiation site are required for proper expression in vivo (1–6, 8, 11, 12, 19, 20). Although upstream elements of individual genes generally contain different nucleotide sequences, they have several features in common which distinguish them from procaryotic promoters. First, these elements act at both long and variable distances from the start site, suggesting that they do not serve as direct polymerase-binding sites. Second, they function in both orientations with respect to the initiation site. Third, they are often the sites for transcriptional regulation.

It is presumed that the regulatory specificity of upstream promoter elements results from their particular DNA sequences and the particular regulatory proteins that interact with them. Nevertheless, if a functional TATA box is present, replacement of an upstream promoter element of a given gene by the upstream region of an unrelated gene results in transcriptional initiation at the proper site. This apparent interchangeability suggests that there is a general mechanism by which upstream promoter elements activate TATA-dependent transcription.

* Corresponding author.

Two general models of upstream promoter function have been suggested. One possibility is that the upstream element acts as an RNA polymerase entry site from which the enzyme can move to its transcriptionally competent binding site. The other possibility is that the upstream elements interact with a protein(s) that allows RNA polymerase to initiate transcription in a TATA-dependent manner. There is little evidence at present to distinguish between these two models.

This paper describes a genetic approach to understanding the nature of upstream promoter elements and their general mechanism of action. The *his3* gene of *Saccharomyces cerevisiae* encodes the histidine biosynthetic gene imidazoleglycerolphosphate (IGP) dehydratase (IGPD). Extensive deletion analysis of the *his3* promoter region identifies an upstream promoter element mapping 113 to 155 base pairs upstream of the transcriptional initiation site (nucleotides −113 to −155) and a TATA element located between −35 and −55 (19, 20). *his3* expression is essential for cell growth only when cells are placed in medium lacking histidine. Yeast strains containing mutations that delete either the upstream or the TATA promoter element fail to express *his3* and are consequently unable to grow unless histidine is added to the growth medium (19, 20). In this study we started with a yeast strain lacking the required *his3* upstream element and selected revertants that are able to grow in the absence of histidine. The rationale is that analysis of such revertants will provide information about the nature of the original mutation and about genes and gene products involved in upstream promoter function.

We isolated mutations that define three different *ope* genes, all of which restored wild-type levels of expression to a *his3* upstream promoter deletion. These *ope* mutations were analyzed for their effects on *his3* transcription and chromatin structure, their pleiotropic effects, and their ability to suppress other *his3* promoter mutations. We discuss

TABLE 1. Strain list

Strain	Genotype	Source or reference
KY103	a *ura3-52 trp1-289 can1 HIS3*$^+$	19
KY162	a *ura3-52 trp1-289 his3*-Δ200 *can1*	19
KY66	KY162 (YRλ21-Sc2782; *TRP1*$^+$ *his3*-Δ13)	19
KY55	KY162 (YRλ21-Sc2755); *TRP1*$^+$ *his3*-Δ16)	19
KY71	KY162 (YRλ21-Sc2639); *TRP1*$^+$ *his3*-Δ4)	19
D536-13A	a *leu2-2,112 his3-11,15 ade1 cyh2 trp1*	J. Szostak
KY516	KY55 *ope1-1*	HIS$^+$ revertant
KY522	KY55 *ope2-1*	HIS$^+$ revertant
KY523	KY55 *ope3-1*	HIS$^+$ revertant
KY570	a *ade1 ura3-52 trp1-289 his3-11,15 leu2-2,112 ope1-1*	KY516 × D536-13A
KY571	α *ade1 ura3-52 trp1-289 his3-11,15 leu2-2,112 ope1-1*	KY516 × D536-13A
KY572	a *ade1 ura3-52 his3-11,15 leu2-2,112 ope2-1*	KY522 × D536-13A
KY573	α *ade1 ura3-52 his3-11,15 leu2-2,112 ope2-1*	KY522 × D536-13A
KY574	a *ura3-52 his3-11,15 leu2-2,112 ope3-1*	KY523 × D536-13A
KY575	α *ade1 his3-11,15 leu2-2,112 ope3-1*	KY523 × D536-13A
KY148	a *ade2 lys2 trp1*-Δ1 *ura3-52 his3*-Δ43	20
KY150	a *ade2 lys2 trp1*-Δ1 *ura3-52 his3*-Δ38	20
KY154	a *ade2 lys2 trp1*-Δ1 *ura3-52 his3*-Δ44	20
KY164	a *ade2 lys2 trp1*-Δ1 *ura3-52 his3*-Δ21	21

some implications concerning upstream promoter elements and the relationship of chromatin structure to transcription and propose models for *ope* function.

MATERIALS AND METHODS

Genetic methods. The genotypes of the yeast strains used in these experiments are listed in Table 1. In general, yeast strains were grown at 30°C in liquid suspension or on 2% Bacto agar plates (Difco Laboratories, Detroit, Mich.) in YPD broth (1% yeast extract, 2% peptone, 2% glucose) or in minimal medium (0.67% yeast nitrogen base [Difco] without amino acids, 2% glucose). When necessary, individual amino acids, uracil, and adenine were added to a concentration of 0.7 mM and Casamino acids were added to 0.3%. Genetic crosses and the analysis of progeny proceeded as follows (23). a and α haploid strains were cross-streaked, and diploids were selected on appropriate medium. Sporulation of diploids was carried out for 3 to 7 days on 2% agar plates containing 2% potassium acetate, 1% yeast extract, and 0.1% glucose. The sporulated culture was incubated in 3% glusulase for 5 to 10 min at room temperature and then placed on ice for 8 to 72 h. Tetrads were dissected under a Zeiss 11 microscope with a micromanipulator (Alan Benjamin Co.) as described by Sherman (18). Spore viability was greater than 90%.

IGPD assays. Enzyme assays were performed by a previous procedure with slight modifications (21). Yeast cells (20 ml) in the exponential phase (A_{600} = 2) were harvested by centrifugation, washed twice in 0.1 M triethanolamine (pH 7.7) (TEA), and suspended in 1 ml of triethanolamine–5 mM 2-mercaptoethanol. These cells were incubated at 37°C for 20 min with 10 μl of chloroform to permeabilize the cell walls; they were then concentrated by centrifugation and suspended in 1 ml of 0.1 M triethanolamine. A 0.8-ml portion of permeabilized cells was added to 0.5 ml of assay buffer such that the final concentrations were 0.1 M triethanolamine, 80 mM 2-mercaptoethanol, and 200 μM $MnCl_2$. A 300-μl aliquot of the reaction mixture was added to each of four microcentrifuge tubes. A 15-μl portion of 0.1 M IGP was added to two tubes, and 15 μl of water was added to the others. These mixtures were incubated at 37°C for 60 min with occasional mixing. The cells were pelleted by centrifugation, and 300 μl of the supernatant was added to 0.7 ml of 1.43 N NaOH. The A_{290} of each tube was measured, and the enzyme level for each strain was determined by the following method. From the mean A_{290} of duplicate tubes containing the total reaction mixture, the mean A_{290} of duplicate tubes without exogenously added IGP was subtracted. A factor representing the inherent A_{290} of the IGP substrate was subtracted. A final adjustment was made to account for the variations in the number of cells assayed (determined by A_{600}). Duplicate points were within ±1%, and enzyme levels are accurate to ±15%.

Preparation and analysis of DNA. Rapid DNA preparations were done as described by Struhl et al. (27). The procedures for synthesizing ^{32}P-labeled DNA probes by nick translation and for hybridization to nitrocellulose filters were described previously (26). To analyze genomic DNA from revertant strains, 0.5 μg of DNA digested with *Eco*RI and *Xho*I was separated electrophoretically in a 0.7% agarose gel, transferred to nitrocellulose, and hybridized to ^{32}P-labeled YRp7-Sc2716 DNA (26) prepared by nick translation.

Preparation and analysis of RNA. The method described below represents a modification of the procedure of Struhl and Davis (25). Cultures of yeast cells (20 ml) grown to the exponential phase were harvested by centrifugation, transferred to a microcentrifuge tube, washed once in 1 M sorbitol, and frozen as a pellet at −80°C. The cells were thawed and then suspended in 0.4 ml of a prewarmed (30°C) solution containing 50 mM potassium phosphate (pH 7.5), 0.95 M sorbitol, 14 mM 2-mercaptoethanol, and 300 U of lyticase. After a 3- to 5-min incubation of the cells at 30°C, sodium dodecyl sulfate and diethylpyrocarbonate were added to 1%, followed immediately by addition of an equal volume of phenol-chloroform-isoamyl alcohol (25:24:1). Total nucleic acid (which contains 99% RNA and will therefore be called total RNA) was prepared by phenol-chloroform extraction and ethanol precipitation. Polyadenylated RNA was prepared by chromatography on oligodeoxythymidylate cellulose as described previously (25).

To measure RNA levels, 5-μg samples of polyadenylated RNA in 50% formamide–2.2 M formaldehyde–20 mM morpholinepropanesulfonic acid buffer (pH 7.0) were heated to 47°C for 15 min. These RNAs were electrophoretically separated in 1.5% agarose gels containing 2.2 M formaldehyde, 20 mM morpholinepropanesulfonic acid (pH 7.0), and 1 mM EDTA. After electrophoresis, the gels were soaked for 30 min in 50 mM NaOH and then for 1 h in 1 M Tris (pH 7.5)–3 M NaCl, transferred to nitrocellulose paper (28), and hybridized with ^{32}P-labeled Sc2676 DNA (23, 26) as described above.

S1 nuclease mapping. In a 1.5-ml microcentrifuge tube, 50 μg of total RNA was mixed with 1 ng of a single-stranded DNA probe in 30 μl of 1 M NaCl–50 mM *N*-2-hydroxyethylpiperazine-*N*′-2-ethanesulfonic acid (pH 7.5).

The hybridization probe extended from nucleotide +174, where it was 5′ end labeled with ^{32}P, to position −134; the specific activity was approximately 10^8 cpm/μg of DNA. Detailed methods for the preparation and purification of this probe will be published elsewhere. The hybridization mixture was incubated for 18 h at 75°C, and it was occasionally spun in the microcentrifuge to avoid excessive evaporation to the top of the tube. After hybridization was complete, 270 μl of buffer (60 mM sodium acetate [pH 4.5], 250 mM NaCl, 1 mM zinc acetate) containing 100 U of S1 nuclease (Sigma Chemical Co., St. Louis, Mo.) was added. After incubation for 30 to 60 min at 37°C, the S1 nuclease digestion was terminated by the addition of 3 μl of 0.5 M EDTA, 1 μl of *E. coli* tRNA (10 mg/ml), and 0.7 ml of ethanol. The nucleic acid was precipitated, washed once with 95% ethanol, and suspended in 10 μl of 0.1 M NaOH–1 mM EDTA. Half of this sample was subjected to electrophoresis as described previously for DNA sequencing (16).

Analysis of chromatin. The mapping of micrococcal nuclease-sensitive sites in chromatin was described previously (22). In brief, osmotically lysed spheroplasts were incubated with an appropriate concentration of micrococcal nuclease for 10 min at 37°C, whereupon DNA was purified by the rapid lysate method (27). This DNA was cleaved with *Hin*dIII, separated in 2% agarose, transferred to nitrocellulose, and challenged for hybridization with ^{32}P-labeled Sc3231 DNA. The probe DNA extends from the *Hin*dIII site at position +335 to an *Eco*RI linker located at nucleotide −134 (22). For the experiment shown in Fig. 6, the adjacent 187-base-pair *Hin*dIII fragment in the *HIS3* structural gene was simultaneously labeled with Sc3231 DNA.

DNA sequencing. The original sources from which *his3*-Δ13 and *his3*-Δ16 were derived are, respectively, the hybrid bacteriophages λgt9-Sc2782 and λgt9-Sc2755 (19). Previously, the *his3* deletion end points were determined to ± 3-base-pair accuracy by a hybridization-S1 nuclease method (19). To determine their precise DNA sequences, appropriate DNA fragments were cloned into single-stranded M13 vectors (13). For λgt9-Sc2782 a *Bgl*II-*Sal*I fragment was cloned into mp19, and for λgt9-Sc2755 an *Eco*RI-*Xho*I fragment was cloned into mp18. DNA sequencing was carried out by the chain termination method (16), except that the primer was a 17-base oligonucleotide corresponding to positions +26 to +42 of the *his3* antisense strand.

RESULTS

Isolation of revertants. The starting strain, *S. cerevisiae* KY66, requires histidine for growth because it contains *his3*-Δ13, an allele which lacks the entire *his3* upstream promoter element but contains the intact TATA element and the entire structural gene (19). The strain was created by integrating a single copy of YRλ21-Sc2782 into the yeast chromosome by homologous recombination at the *trp*I locus on chromosome IV (Fig. 1). This allele, which is tightly linked to a selectable Trp^+ marker, represents the only *his3* information present in the cell, because the normal *his3* locus on the chromosome was deleted by the *his3*-Δ200 mutation.

Previously, hybridization-S1 nuclease mapping indicated that the *his3* deletion breakpoint of Δ13 was located at nucleotide −63 ± 3 (19). DNA sequencing of λgt9-Sc2782, the initial source of *his3*-Δ13, demonstrates that the actual endpoint is at position −66 (see above). However, this DNA sequence analysis also indicates that the structure of λgt9-Sc2782 is more complex than was originally suspected (Fig. 1). Since this phage was obtained as a spontaneous deletion

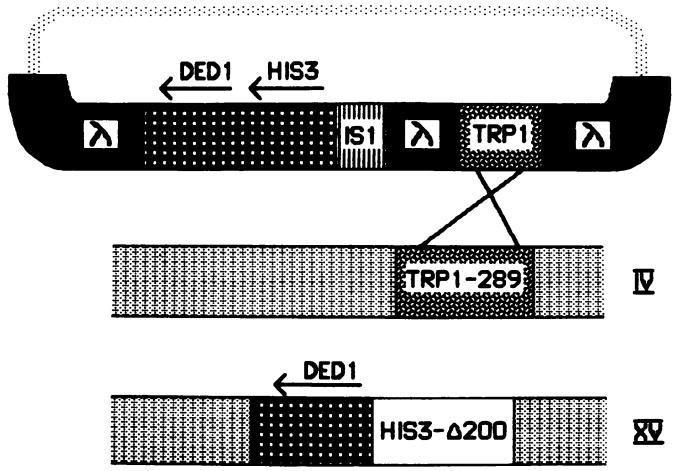

FIG. 1. Origin of *S. cerevisae* KY66 (*his3*-Δ13). The top part of the figure shows the structure of YRλ21-Sc2782 (not to scale). It indicates both the linear form found in λ phage particles and the circular form found in yeast cells. DNA from the yeast *ded1-his3* and *trp1* gene regions as well as the *E. coli* IS*1* insertion element are indicated (see text). This molecule can replicate autonomously in yeast cells owing to the *ars1* sequence adjacent to the *trp1* structural gene. The bottom part of the figure indicates chromosomes IV (containing the *trp1-289* mutation) and XV (containing the *his3*-Δ200 deletion) from strain KY162. Chromosomal sequences homologous to YRλ21-Sc2782 are indicated by their original pattern in the top part of the figure, whereas adjacent but nonhomologous genomic regions are indicated by unlabeled, stippled bars. *S. cerevisiae* KY66 was obtained by homologous recombination between YRλ21-Sc2782 and the chromosomal *trp1* locus.

mutant of the λ *his3* phage, λgt9-Sc2601, it was expected that the sequences immediately upstream of position −66 would correspond to λ sequences. Surprisingly, the adjacent sequences correspond exactly to the left end of the *E. coli* IS*1* insertion element (14). Restriction mapping of λgt9-Sc2782 DNA strongly suggests that the entire IS*1* element is still present and that the deletion breakpoint within the λ sequence occurs approximately at nucleotide 32000 (17). From these observations, we suggest that λgt9-Sc2782 arose by IS*1* insertion into position −66 of the original phage, followed by an IS*1*-mediated deletion event.

Cultures of *S. cerevisiae* KY66 were grown in broth and plated on minimal medium lacking histidine. His^+ revertants were obtained at a frequency of 10^{-6}, and 23 revertants of independent origin were chosen for further study. These 23 strains were mated to strain D536-13A (23), and the resulting diploids were tested for their ability to grow on minimal medium plates lacking histidine. Three diploids were His^+, indicating that these revertants were due to dominant mutations. Tetrad analysis of the progeny of these crosses showed that the His^+ phenotype segregated 2:2 in all tetrads and that all His^+ spores were Trp^+. Analysis of genomic DNA of the revertants with dominant mutations showed chromosomal rearrangements at the *his3* locus (data not shown); these revertants were not studied further. The remaining 20 diploids were His^-, thus suggesting that the original revertants were due to recessive mutations. Analysis of tetrads from one such His^- diploid showed that only 25% of the progeny were His^+. Furthermore, only 50% of the Trp^+ progeny were His^+, thus confirming that a recessive suppressor mutation in a single gene is responsible for the His^+ phenotype. This gene is termed *ope1* (*o*verrides *p*romoter *e*lement). Finally, 25% of the progeny were geno-

TABLE 2. Growth properties[a]

Strain	Doubling time (h) on:		Growth at 37°C	Crunchy morphology[b]
	YPD medium	Minimal medium		
KY103 (wild type)	2	2	+	−
KY516 (*ope1*)	2	3.5	−	++
KY522 (*ope2*)	2	3	+	+
KY523 (*ope3*)	2	4.5	−	+++

[a] Doubling times for strains KY103, KY516, KY522, and KY523 grown at 30°C in YPD broth or in glucose minimal medium are measured in hours. *ope1* and *ope3* mutants are unable to grow at 37°C in either medium.

[b] The presence of each of the *ope* mutations results in an abnormal, crunchy colony morphology of varying severity as indicated by the number of pluses (Fig. 2); wild-type cells are smooth, as indicated by a minus sign.

typically *his3*$^-$ *ope1-1* and phenotypically His$^-$. This demonstrates that the *ope1-1* mutation does not simply bypass the need for the *his3* product and that *ope1* is unlinked genetically to *his3*.

The suppressor mutations were placed into complementation groups in the following way. The His$^+$ revertants were crossed to KY530 (a *ope1-1 his3*-Δ13). A total of 17 revertants gave His$^+$ diploids, indicating that they also contain *ope1* mutations. The remaining three revertants gave His$^-$ diploids, indicating that the suppressor mutations were not allelic to *ope1*. By applying the same analysis to the remaining revertants, we identified two more complementation groups, *ope2* (two alleles) and *ope3* (one allele). Revertants due to *ope2* or *ope3* mutations were then crossed to strain D536-13A. Tetrad analysis similar to that described for *ope1* indicated that *ope2* and *ope3* mutations defined single genes unlinked to *his3*. In summary, recessive mutations in any of three unlinked *ope* genes all suppress the phenotype conferred by the *his3*-Δ13 allele.

Phenotypes caused by *ope* mutations. Suppressor mutations might be expected to confer pleiotropic effects if they affect some general aspect of gene expression. Indeed, mutations in each of the *ope* genes confer recessive phenotypes in the absence of a suppressible *his3* allele (Table 2). *ope* mutations cause a crunchy colony morphology such that the entire colony comes off the agar when it is replica plated (Fig. 2). In liquid medium, large flakes are formed which do not go readily into solution and which do not form a pellet after centrifugation. Mutations in *ope3* are associated with the most severe morphological effects; those of *ope2* are associated with the least. Further, mutations in the *ope1* or *ope3* genes cause failure to grow at 37°C. This temperature-sensitive lethality is apparently the result of osmotic instability, since strains containing these mutations lyse at the restrictive temperature unless 1 M sorbitol is added to the medium. *ope* mutations also cause slower growth rates in minimal medium. At 30°C, the wild-type parent doubles every 2 h, whereas the doubling times for *ope3*, *ope1*, and *ope2* strains are 4.5, 3.5, and 3 h, respectively. This slowed growth is not observed in rich medium or in minimal medium supplemented with Casamino acids. It may be related to another pleiotropic effect, namely that *ope3* and *ope1* strains grow extremely poorly in liquid medium with added histidine. Thus, it is possible that the slowed growth rates are due to the presence of the histidine that the cells are producing.

The unusual colony morphologies described above resemble those caused by *cyc8* and *cyc9* mutations (15). Furthermore, *cyc8* and *cyc9* mutations increase the expression level of the minor cytochrome *c* isozyme (encoded by *cyc7*). Thus, these *cyc* mutations are similar to the *ope* mutations in that they increase the expression of unlinked genes. However, the *ope* mutations are not alleles of the *cyc8* or *cyc9* genes. First, the *ope* mutations are unlinked to *lys2*, whereas *cyc8* is tightly linked (15). Second, *cyc9* mutants mate very poorly as α strains, and homozygous *cyc9* diploids do not sporulate (15); *ope* mutants do not have any of these properties. Third, *ope* mutants fail to grow at high temperatures, unlike *cyc8* or *cyc9* mutants.

Effect of the suppressors on *his3* expression. The increase in the level of expression of the *his3* gene product resulting from the suppressor mutations was quantified by assaying the activity level of IGPD. Cultures were grown in broth and minimal medium. As shown previously, the wild-type strain had IGPD activity at the basal level in both growth media, whereas the *his3*-Δ13 strain produced little, if any, enzy-

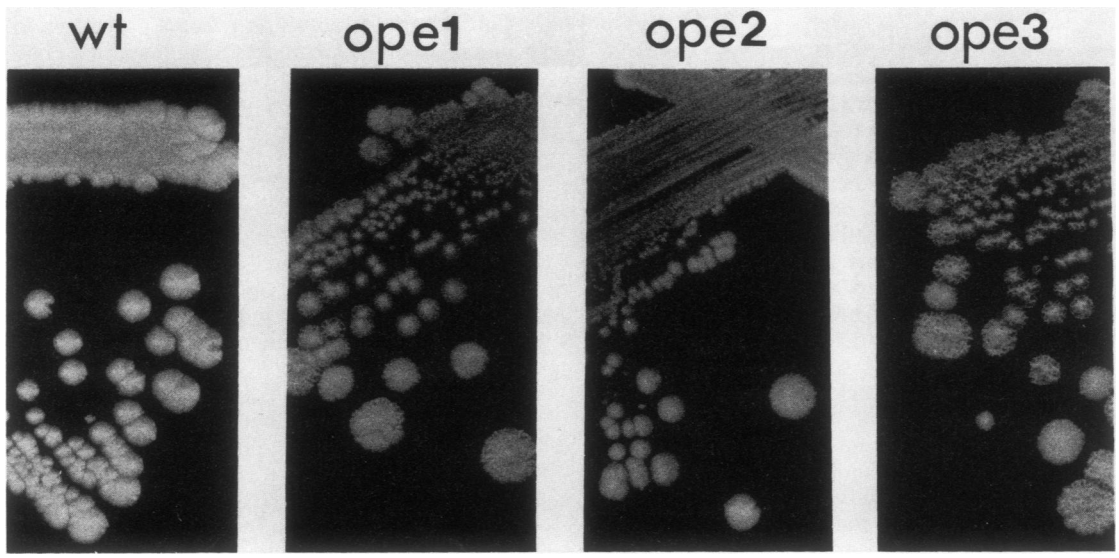

FIG. 2. Colony morphology of *ope* strains.

matic activity under either condition (19, 21). As expected, when the cultures were grown in minimal medium, the presence of the *ope1*, *ope2*, and *ope3* mutations increased the level of IGPD activity to approximately the wild-type levels (Table 3). The relative levels of IGPD activity, with *ope3* producing the most and *ope2* producing the least, correlates well with the degree of suppression as indicated by the relative severity of the pleiotropic effects. Surprisingly, unlike the situation for wild-type strains, no IGPD activity was observed for the three *ope* suppressor-containing strains when grown in YPD broth.

The regulation is a function neither of the different growth rates exhibited by the revertants nor of the presence of histidine. Strains growing in minimal medium with or without histidine plus Casamino acids grow at the same rate as they do in broth, yet still make wild-type levels of IGPD. Instead, some component of the rich medium seems to prevent *his3* expression. Suppressor strains grown in medium that is 25% YPD–75% minimal do not have detectable levels of IGPD activity.

The observation that *ope* mutations suppress the upstream promoter deletions in a regulated manner is unexpected for several reasons. First, the regulation observed is not the same as seen for a wild-type *his3* gene. A wild-type *his3* gene produces the basal level of IGPD in both rich and minimal media (Table 3). Normal induction of the *his3* gene or any coordinately regulated gene is achieved only when cells are starved by metabolic poisons. Second, sequences located between −100 and −83 are required for regulation of the *his3* gene, yet these are deleted in *his3*-Δ13 (21). Third, when the *his3*-Δ13 parent strain is placed in minimal medium lacking histidine, the cells are clearly starving for this amino acid and should be undergoing the starvation response. Thus, since *his3*-Δ13 does not cause *his3* expression even under starvation conditions, the *ope* effect must be due to something else.

Effects of *ope* mutations on *his3* transcription. The effect of the suppressors on *his3* expression can be seen at the RNA level (Fig. 3). Total and polyadenylated RNA were analyzed with a hybridization probe consisting of DNA that includes the entire *his3* gene and parts of the adjacent yeast genes *ded1* and *pet56* (to provide internal standards for quantifying RNA levels). Although IGPD activity was not detected from KY66, faint bands of *his3* RNA are visible on the autoradiogram (Fig. 3). As expected from the IGPD assays, the levels of RNA in suppressor strains grown in broth are comparable to those in KY66, whereas the strains grown in minimal medium have approximately wild-type levels of RNA.

TABLE 3. IGPD levels[a]

Strain	Genotype	IGPD levels for growth in:	
		Complete (YPD) medium	Minimal medium
KY103	Wild type	1.0	1.0
KY66	Δ13	<0.1	0.1
KY516	Δ13, *ope1*	<0.1	1.1
KY522	Δ13, *ope2*	<0.1	0.4
KY523	Δ13, *ope3*	<0.1	1.5

[a] Yeast strains were grown in YPD or in minimal medium lacking histidine (histidine was added to the culture of KY66, which requires it for growth). The levels of IGPD (the *his3* gene product) are presented as relative to that of a wild-type yeast (defined as 1.0) grown in YPD medium. Enzyme activity values are accurate within 15%.

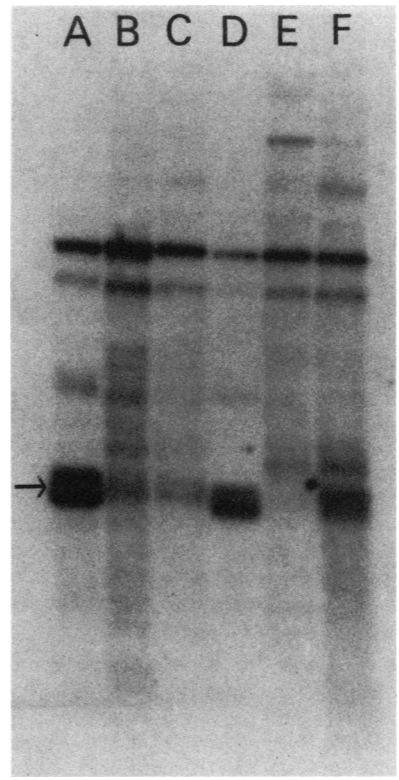

FIG. 3. RNA levels in *ope* mutants. Polyadenylated RNA was prepared from strains grown in YPD medium (lanes A [strain KY103, wild type], B [strain KY66, *his3*-Δ13], and C [strain KY522, *his3*-Δ13, *ope1*]) or in minimal medium (lanes D [strain KY103], E [strain KY66], and F [strain KY522]). These RNAs (5 μg per lane) were hybridized to ^{32}P-labeled Sc2676 DNA. The arrow indicates the position of the *his3* message, which for unknown reasons usually appears as a doublet. The uppermost bands in all the lanes represent transcripts of the *ded1* gene, which in the genome is adjacent to *his3* (25; K. Struhl, unpublished results). Lanes A and D also contain a band corresponding to the 1.2-kilobase transcript of the *pet56* gene, which is also adjacent to *his3*; 200 base pairs of this RNA species are represented in the probe. This transcript is not visible in lanes B, C, E, or F because the *his3*-Δ200 mutation reduces *pet56* transcription by a factor of 5 (K.Struhl, unpublished results).

If the suppressors are indeed supplying the function of the upstream element or supplanting the need for it, the *his3* transcriptional initiation sites should be the same as in the wild-type gene. The wild-type *his3* gene has two major transcription start sites, located at nucleotides +1 and +12, and a minor site at +22 (24).

The 5′ ends were mapped by hybridizing RNA to a single-stranded DNA probe and treating the resulting duplexes with S1 nuclease (Fig. 4; see above). As expected, proper transcription was observed only in minimal media. Surprisingly however, the *ope* suppressors only restore transcription initiated at +12 and +22. Bands corresponding to readthrough transcription from the IS*1* or λ sequences are also visible in both the starting His$^-$ strain and the His$^+$ revertants when grown in both rich and minimal media. These readthrough transcripts probably account for the heterogeneous RNA species visible in Fig. 3 (lanes B, C, E, and F). However, since no IGPD activity is detected except in *ope* strains in minimal medium, it is likely that these readthrough transcripts are not translated into functional *his3* product. This is strongly supported by the fact that all

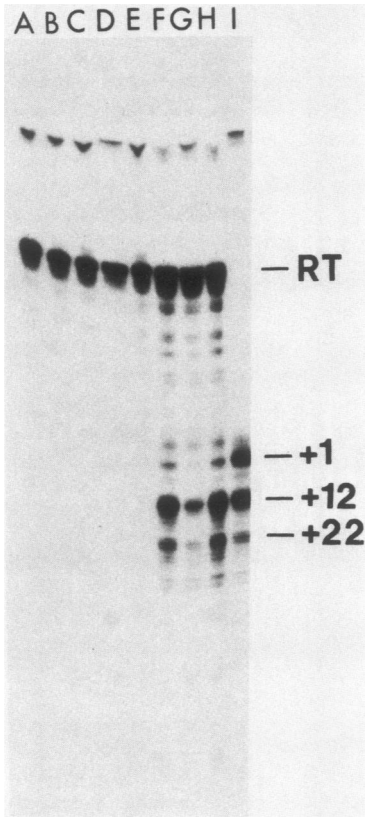

FIG. 4. 5′ mapping of RNA transcripts. Total RNA was hybridized to a single-stranded *his3* probe and treated with S1 nuclease (see text). RNAs were prepared from cells grown in YDP (lanes A through D) or in minimal medium (lanes E through I), with strains KY66 (*his3*-Δ13; lanes A and E), KY516 (Δ13, *ope1*; lanes B and F), KY522 (Δ13, *ope2*; lanes C and G), KY523 (Δ13, *ope3*; lanes D and H), and KY103 (wild type; lane I). *his3* transcripts that initiate from nucleotides +1, +12, and +22 as well as readthrough transcripts (RT) initiating upstream of nucleotide −66 are indicated.

readthrough transcripts that begin in the flanking DNA sequences contain AUG codons that are upstream of the correct initiation codon and that specify the incorrect reading frame for the *his3* product (26).

Effect of *ope* mutations on *his3* chromatin structure. The TATA box of the wild-type *his3* gene is preferentially sensitive to cleavage by micrococcal nuclease (22). Deletion of the upstream promoter element as in *his3*-Δ13 results in decreased sensitivity of the TATA box to micrococcal nuclease digestion (22). From this result, it has been suggested that the upstream element might be necessary for setting up the "correct" chromatin structure at the TATA box so that transcription could be initiated. In this light, one class of mutations that might be expected to restore *his3* expression are those which arrange the chromatin in the wild-type transcriptionally active configuration.

The chromatin structures of the His^+ revertants were assayed by micrococcal nuclease digestion. The TATA box sensitivity in the revertant strains is indistinguishable from the *his3*-Δ13 parent. This result is obtained in rich medium, when *his3* is not expressed (Fig. 5), and in minimal medium, when *his3* is expressed at wild-type levels (Fig. 6). Thus, as measured by this assay, the *ope* mutations do not appear to restore the wild-type chromatin configuration, even though *his3* transcription at a correct initiation site is restored.

***his3* allele specificity of *ope* suppressors.** The effect of the *ope* mutations on other *his3* alleles with various promoter defects was examined by constructing the appropriate double mutants (Fig. 7; Table 4). *ope* mutations do not suppress the phenotype of *his3*-Δ38, *his3*-Δ43, *his3*-Δ44, or *his3*-Δ21, all of which lack the TATA box but not the upstream promoter region (20). Moreover, *his3*-Δ4, which deletes all sequences upstream of −11 and thus lacks both the upstream region and the TATA box (26), is not suppressed. These results are in keeping with the view that suppressors can promote TATA-dependent transcription but cannot substitute for the TATA element. The effect of each of the three *ope* suppressors on another upstream promoter deletion was also considered. Mutations in *ope1*, *ope2*, and *ope3* do not suppress the phenotype of *his3*-Δ16, which deletes all sequences upstream of −96, but contains flanking sequences from another region of λ DNA than those present in *his3*-Δ13 (see legend to Fig. 7). Thus, the *ope* suppressor mutations are highly allele specific in that they only suppress *his3*-Δ13, the allele used to isolate them.

***ope* double mutants.** Haploid His^+ colonies containing *his3*-Δ13 and one of the *ope* suppressor mutations were mated in all possible combinations. Analysis of the resulting diploids showed that the frequency of tetrads with four viable spores was as high as seen for standard crosses, thus

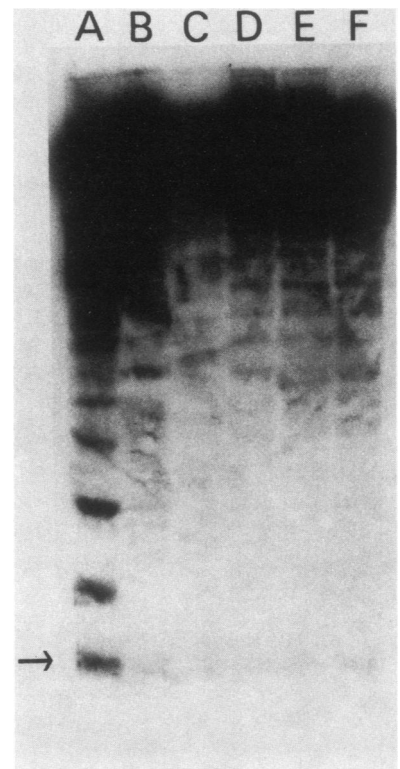

FIG. 5. Chromatin structure in strains grown in YPD medium. Bands of hybridization indicate micrococcal nuclease cleavage sites in chromatin prepared from cells grown in YPD medium. Lanes A, strain KY103 (wild type); B, strain KY66 (Δ13); C, strain KY55 (Δ16); D, strain KY516 (Δ13, *ope1*); E, strain KY522 (Δ13, *ope2*); and F, KY523 (Δ13, *ope3*). The arrow indicates the position of micrococcal sensitivity at the TATA box as determined previously by high-resolution mapping (22). Other bands in lane A indicate cleavage in the yeast genomic sequences upstream of the *his3* gene; these sequences are deleted in Δ13 and Δ16.

suggesting that strains containing two *ope* mutations are equally viable as singly mutant strains. Furthermore, double mutants, which were identified by their inability to complement strains with either one of the relevant *ope* mutations, were obtained at the expected frequency of 25%. This indicates that the double mutants are indeed equally viable and that all the three *ope* genes are unlinked to each other. Standard linkage analysis to the centromere-linked markers *ura3* and *trp1* indicate that all *ope* genes are unlinked genetically to any centromere. The phenotypes of all the double mutants are indistinguishable from those of the single mutants in terms of pleiotropic effects and *his3*-Δ13 suppressibility.

DISCUSSION

Some observations concerning *his3* expression. Suppressor mutations in three different *ope* genes restore wild-type levels of expression to a *his3* promoter mutant that lacks the upstream element. Suppression is observed only under certain physiological conditions and in all cases is due to increased *his3* transcription, which begins at a normal *his3* initiation site. One initially surprising observation was that the transcription mediated by the *ope* suppressors was initiated from only one of the two normal *his3* initiation sites. Transcription of the wild-type *his3* gene is initiated about equally from the +1 and +12 sites, whereas transcription due to the *ope* mutations is initiated primarily at the +12 site and somewhat at the normally minor +22 site. This unusual pattern of initiation sites was also observed when the *gal1,10* upstream regulatory site is substituted for the *his3* upstream promoter region (24). This result adds support to the suggestion that there may be different kinds of upstream promoter elements: those that promote initiation at +1 and +12 and those that only promote initiation at +12. Thus, although it is apparent that there are common features by which different upstream promoter elements potentiate TATA-

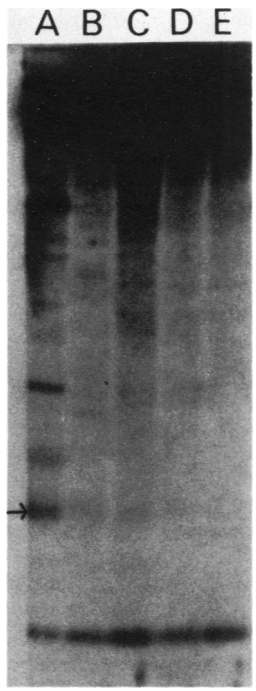

FIG. 6. Chromatin structure in strains grown in minimal medium. The experiment is the same as that shown in Fig. 4, except that cells were grown in minimal medium. In addition, the hybridization probe was made by nick translating a mixture of Sc3231 DNA and the adjacent 187-base-pair *Hin*dIII fragment in the *his3* structural gene; this provides an internal control for the amount of DNA loaded in each lane. Lanes: A, strain KY103 (wild type); B, strain KY66 (Δ13); C, strain KY516 (Δ13, *ope1*); D, strain KY522 (Δ13, *ope2*); and E, strain KY523 (Δ13, *ope3*). The arrow indicates the position of micrococcal sensitivity at the TATA box (22), and the band below the TATA box position represents hybridization to the 187-base-pair *Hin*dIII fragment.

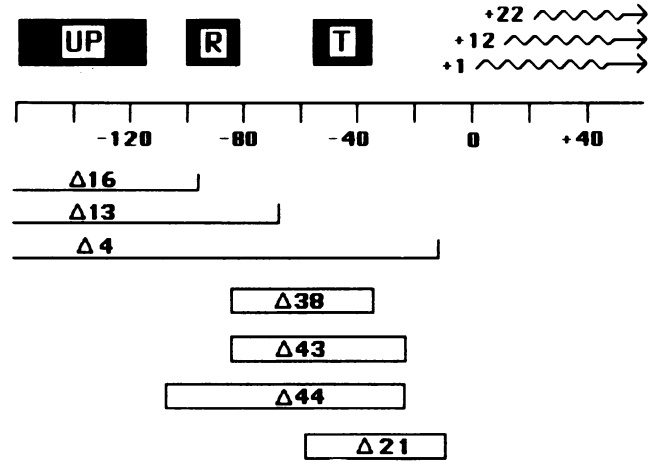

FIG. 7. Structure of the *his3* promoter region and promoter mutants. At the top of the figure, black boxes indicate the positions of TATA box (T), located between −35 and −55, regulatory element (R), located between −83 and −99, and the upstream promoter element (UP), located between −113 and −155 (nucleotide numbers are defined with respect to the site of transcriptional initiation). *his3* transcripts initiating at positions +1, +12 (major sites) and +22 (minor site) are shown as wavy lines. The structures of deletion mutants (19 through 21) used in the allele specificity experiments are shown below. Vertical lines indicate the *his3* breakpoints of λ *his3* deletion alleles Δ16 (to −96), Δ13 (to −66), and Δ4 (to −11). The breakpoints within the λ DNA sequence (16) are at nucleotide 26945 for Δ16 and nucleotide 27735 for Δ4. The flanking sequences in *his3*-Δ13 are from the IS1 insertion element (see Fig. 1 and text). Open boxes indicate the extent of internal deletions Δ38 (−83 to −35), Δ43 (−83 to −35), Δ44 (−109 to −24), and Δ21 (−59 to −9).

TABLE 4. Allele specificity[a]

his3 allele	Endpoints		ope genotype[b]			
	Upstream	Downstream	*OPE*⁺	*OPE1*	*OPE2*	*OPE3*
Wild type	None	None	+	+	+	+
Δ13	λ	−66	−	+	+	+
Δ16	λ	−96	−	−	−	−
Δ4	λ	−11	−	−	−	−
Δ38	−83	−35	(−)	(−)	(−)	(−)
Δ43	−83	−24	(−)	(−)	NT[c]	(−)
Δ44	−109	−24	(−)	(−)	NT	(−)
Δ21	−59	−9	(−)	(−)	NT	(−)

[a] Double mutants containing eight different *his3* alleles (rows) and *ope* alleles (columns), are listed in matrix form. The *his3* endpoints of these deletion alleles are indicated (see Figure 7 for a diagrammatic view).

[b] Histidine expression of these double mutants was determiend by replica plating onto plates lacking histidine: +, wild-type growth; −, that no visible growth was observed; (−), faint growth response.

[c] NT, Not tested.

dependent transcription, there also seem to be different general classes.

One concern with the experiments described here was that readthrough transcription from the fused IS*1* or λ sequence would interfere with the initiation of proper transcription. Indeed, 5′ mapping of the RNA from a *his3*-Δ13 strain shows that there is considerable readthrough transcription. However, these transcripts are obviously not translated into a functional *his3* gene product, because the strain is His^-. The amount of readthrough transcription appears unchanged in the His^+ revertants under conditions when proper *his3* transcripts are being made (minimal media) and those when they are not (broth). Thus, the readthrough transcription does not appear to interfere with the ability to obtain revertants of *his3*-Δ13 that restore the proper *his3* transcript.

Relationship of chromatin structure to *his3* transcription. Micrococcal nuclease digestion of nuclear chromatin indicates that the *his3*-Δ13 allele has a different chromatin structure from that of the wild-type *his3* gene (22). Thus, analysis of the *ope* revertants provides an opportunity to consider the relationship of chromatin structure to *his3* expression. The chromatin structure of each His^+ revertant appears unchanged from that of the His^- parent, even though a wild-type basal level of *his3* mRNA is being produced. A similar result was obtained when the *gal1,10* upstream regulatory site replaces the *his3* upstream promoter element (K. Struhl, unpublished results). Despite the very high levels of transcription that occur when such strains are grown in galactose-containing medium, the normal TATA box sensitivity is not restored. Thus it is apparent that TATA box sensitivity to micrococcal nuclease cleavage is not correlated with transcriptional activation. It is possible that the TATA hypersensitivity of the wild-type gene is related to transcription initiated at the +1 site, because transcription dependent on the *ope* mutations or on the *gal1,10* element is initiated only from +12.

Models for *ope* suppression. In principle, there are several ways in which mutations in unlinked genes could restore *his3* expression to a mutant allele lacking the upstream promoter element. First, if the upstream promoter element organizes an active chromatin structure that permits TATA-dependent transcriptional initiation, a suppressor mutation causing the chromatin to be always in a transcriptionally active state might bypass the need for the upstream element. Second, a mutation in a gene whose product interacts with some upstream promoter sequence could permit the altered protein to recognize other sequences that are present in the mutant *his3* allele. Third, a mutation could cause some physiological alteration which changes the efficiency of a cryptic promoter element present in the original mutant allele.

Since the *ope* mutations suppress the His^- phenotype of one *his3* upstream promoter mutation (*his3*-Δ13) but not of another very similar allele (*his3*-Δ16), it seems unlikely that the *ope* mutations are acting by a general mechanism that bypasses the necessity of the upstream element.

The second hypothesis would explain the results as follows. *ope* genes encode DNA-binding proteins, and the mutations described here alter the proteins such that they now recognize a sequence present in *his3*-Δ13 but not in *his3*-Δ16. The wild-type *ope* gene products are normally involved in the expression of other genes; hence the pleiotropic effects caused by the mutations. Furthermore, the *ope* products are regulatory proteins such that functional interactions with the relevant DNA sequences only occur in minimal medium. Clearly, the *ope* gene products are required in both rich and minimal media as the pleiotropic effects caused by *ope* mutations persist under both conditions.

Two observations argue against this interpretation. First, many different alleles of *ope1* and *ope2* were obtained, and it is hard to imagine that each was altered in such a way as to only recognize sequences in *his3*-Δ13 but not in *his3*-Δ16. Instead, the high frequency of mutation (10^{-6}), the large number of alleles obtained, and the recessive nature of the mutation all suggest that the suppression is due to the loss of function of the *ope* gene products. Second, it would be surprising if mutations in three different genes involved in upstream promoter function all cause the same pleiotropic effects.

In light of these objections, we favor the third interpretation, namely that the utilization of a cryptic upstream promoter element is increased by altering the metabolism of the cell. In this model, something in the IS1 or λ sequence that is fused to the *his3* structural gene in *his3*-Δ13 would contain a cryptic upstream promoter element that resembles the upstream promoter element for a particular class of genes (arbitrarily called class X). Under normal circumstances, this cryptic promoter is not used; if it were, the starting mutant would not be his^-. However, when physiological conditions are altered by the *ope* mutations, the cell responds by inducing transcription of class X genes. Thus, transcription of *his3*-Δ13 is also increased, because fortuitously it is a class X gene by virtue of its related upstream sequence. Viewed in this fashion, it is not surprising that mutations in all three *ope* genes confer the same phenotypes. Rather than being incidental effects associated with altered transcription patterns, the crunchy colony morphology, the temperature sensitivity, and the osmotic instability would be manifestations of the physiological defect. The observed allele specificity is also explained by this model as the nucleotide sequence for the cryptic promoter element could be present (and close enough to the TATA box) in *his3*-Δ13 but not in *his3*-Δ16.

If the above explanation is correct, the *ope* genes could be involved at almost any stage of cellular metabolism. One specific suggestion is that the *ope* genes might encode enzymes involved in the biosynthesis of a particular compound called X; *ope* mutants therefore would produce insufficient amounts of compound X. By analogy with many metabolic pathways, the cells would induce the X genes to try to synthesize more compound X. The observed regulation by the *ope* suppressors could be explained by the presence of compound X in broth (which would prevent induction of the X genes) and its absence from minimal medium. The physiological alterations suggest that such a compound might be a precursor to cell wall biosynthesis.

Implications concerning upstream promoter elements and reversion experiments. If the cryptic promoter element model is indeed the correct explanation, it might appear that the experiments reported here represent an unusual and unfortunate situation. However, this model also easily explains data that we and others have obtained in other reversion experiments. Our attempts to revert the *his3*-Δ16 allele yielded a large number of spontaneous revertants in at least 15 complementation groups. Again, as with the *his3*-Δ13 revertants, these were allele specific. Miles Chang, in this laboratory, obtained revertants of *his3*-Δ4X (a derivative of *his3*-Δ4), which define at least three complementation groups, all unrelated to previous ones. Similarly, Mark Johnston (personal communication) reverted a *gal1* mutation in which the upstream promoter element was inactivated and

obtained many revertants which defined a large number of complementation groups. Thus, despite a priori expectations, it is rather easy to revert promoter deletions by unlinked suppressor mutations. The large number of genes defined by such mutations is difficult to explain if all the mutations are thought to be in proteins involved in gene expression. It seems more likely that one or several cryptic promoter elements are present upstream in each of these deletion alleles, and that "metabolic" mutations alter the efficiency with which they are used. Unlike the large number of mutant genes in these other reversion experiments, the small number of *ope* genes, the obvious nature of the physiological defect, and the unexpected regulation makes it easier to conclude that cryptic upstream promoter elements are a general phenomenon.

Any deletion brings in new sequences, whether from foreign DNA (as in *his3*-Δ13) or from the same organism (an internal deletion). Since it was demonstrated that sequences as far as 1 kilobase upstream act as promoter elements or regulatory sites, or both, and that such sequences act at variable distances and in both orientations (1, 4, 6, 8, 12, 24), any sequence within this new 1-kilobase region is a potential promoter element. The ease of reverting different promoter deletions suggests that the frequency of finding cryptic promoter elements is rather high. To account for this high frequency, it follows that upstream promoter elements are composed of short sequences. Moreover, this interpretation also suggests that cryptic promoter elements are present throughout the genome. In normal strains such elements should have no effect on transcription, because they are isolated from other required promoter elements. However, genomic rearrangements could bring the cryptic sequences into functional association with the promoter region of a particular gene, thereby placing that gene under the control of a new promoter-regulatory element. Thus, in evolutionary terms, this reservoir of cryptic elements provides a mechanism for altering specific patterns of gene regulation.

ACKNOWLEDGMENTS

We thank Stewart Scherer and Mark Johnston for communication of results before publication and for fruitful discussions.

This work was supported by a grant from the Searle Scholars Program and Public Health Service grant GM30186 from the National Institutes of Health.

LITERATURE CITED

1. **Banerji, J., S. Rusconi, and W. Schaffner.** 1981. Expression of a β-globin gene is enhanced by remote SV40 DNA sequences. Cell **27**:299–308.
2. **Benoist, C., and P. Chambon.** 1981. *In vivo* sequence requirements of the SV40 early promoter region. Nature (London) **290**:304–310.
3. **Breathnach, R., and P. Chambon.** 1981. Organization and expression of eukaryotic split genes coding for proteins. Annu. Rev. Biochem. **50**:349–383.
4. **Chandler, V. L., B. A. Maler, and K. R. Yamamoto.** 1983. DNA Sequences bound specifically by glucocorticoid receptor *in vitro* render a heterologous promoter hormone responsive *in vivo*. Cell **33**:489–499.
5. **Dierks, P., A. VanOoyen, N. Mantei, and C. Weissman.** 1981. DNA sequences preceding the rabbit β-globin gene are required for the formation of β-globin RNA with the correct 5′ terminus in mouse L cells. Proc. Natl. Acad. Sci. U.S.A. **78**:1411–1415.
6. **Fromm, M., and P. Berg.** 1982. Deletion mapping of DNA regions required for SV40 early promoter function *in vivo*. J. Mol. Appl. Genet. **1**:457–481.
7. **Grosveld, G. C., C. K. Shewmaker, P. Jat, and R. A. Flavell.** 1981. Location of DNA sequences necessary for transcription of the rabbit β-globin gene *in vitro*. Cell **25**:215–226.
8. **Guarente, L., R. R. Yocum, and P. Gifford.** 1982. A *GAL10-CYC1* hybrid yeast promoter identifies the *GAL4* regulatory region as an upstream site. Proc. Natl. Acad. Sci. U.S.A. **79**:7410–7414.
9. **Hawley, D. K., and W. R. McClure.** 1983. Compilation and analysis of *Escherichia coli* promoter DNA sequences. Nucleic Acids Res. **11**:2237–2255.
10. **Mathis, D., and P. Chambon.** 1981. The SV40 early region TATA box is required for accurate *in vitro* initiation of transcription. Nature (London) **290**:310–315.
11. **McKnight, S. L., and R. Kingsbury.** 1982. Transcriptional control signals of a eukaryotic protein coding gene. Science **217**:316–324.
12. **Moreau, P., R. Hen, B. Wasylyk, R. Everett, M. P. Gaub, and P. Chambon.** 1981. The SV40 72 base pair repeat has a striking effect on gene expression both in SV40 and other chimeric recombinants. Nucleic Acids Res. **9**:6047–6048.
13. **Norrander, J., T. Kempe, and J. Messing.** 1983. Improved M13 vectors using oligonucleotide mutagenesis. Gene **26**:101–106.
14. **Ohtsubo, E., and H. Ohtsubo.** 1978. Nucleotide sequence of an insertion element, IS1. Proc. Natl. Acad. Sci. U.S.A. **75**:615–619.
15. **Rothstein, R. J., and F. Sherman.** 1979. Genes affecting the expression of cytochrome c in yeast: genetic mapping and genetic interactions. Genetics **94**:871–889.
16. **Sanger, F., A. R. Coulson, B. G. Barell, A. J. Smith, and B. A. Roe.** 1980. Cloning in single-stranded bacteriophage as an aid to rapid DNA sequencing. J. Mol. Biol. **143**:161–178.
17. **Sanger, F., A. R. Coulson, G. F. Hong, D. F. Hill, and G. B. Petersen.** 1982. Nucleotide sequence of bacteriophage λ DNA. J. Mol. Biol. **162**:729–773.
18. **Sherman, F.** 1973. Micromanipulator for yeast genetic studies. Appl. Microbiol. **26**:829.
19. **Struhl, K.** 1981. Deletion mapping a eukaryotic promoter. Proc. Natl. Acad. Sci. U.S.A. **78**:4461–4465.
20. **Struhl, K.** 1982. The yeast *his3* promoter contains at least two distinct elements. Proc. Natl. Acad. Sci. U.S.A. **79**:7385–7389.
21. **Struhl, K.** 1982. Regulatory sites for *his3* expression in yeast. Nature (London) **300**:284–287.
22. **Struhl, K.** 1982. Promoter elements, regulatory elements, and chromatin structure of the yeast *his3* gene. Cold Spring Harbor Symp. Quant. Biol. **47**:901–910.
23. **Struhl, K.** 1983. Direct selection for gene replacement events in yeast. Gene **26**:231–242.
24. **Struhl, K.** 1984. Genetic properties and chromatin structure of the yeast *gal* regulatory element: an enhancer-like sequence. Proc. Natl. Acad. Sci. U.S.A. **81**:7865–7869.
25. **Struhl, K., and R. W. Davis.** 1981. Transcription of the *his3* gene region of *Saccharomyces cerevisiae*. J. Mol. Biol. **152**:535–552.
26. **Struhl, K., and R. W. Davis.** 1981. Promoter mutants of the yeast *his3* gene. J. Mol. Biol. **152**:553–568.
27. **Struhl, K., D. T. Stinchcomb, S. Scherer, and R. W. Davis.** 1979. High frequency transformation of yeast: autonomous replication of hybrid DNA molecules. Proc. Natl. Acad. Sci. U.S.A. **76**:1035–1039.
28. **Thomas, P. S.** 1980. Hybridization of denatured RNA and small DNA fragments transferred to nitrocellulose. Proc. Natl. Acad. Sci. U.S.A. **77**:5201–5205.